Letters in Applied NanoBioScience
Open-Access Journal (ISSN: 2284-6808)

Article
Volume 12, Issue ..., 2026, ...
https://doi.org/10.33263/LIANBS120.000

Probing the interaction mechanisms of organophosphate pesticide Profenofos with Diabetes associated proteins: Molecular Docking and ADME-Toxicity studies

Manojkumar Muthupandi [1], Azar Zochedh [2,*], Mohana Priya [3,4], Naveen Kumar Muthupandi [5], Amirthavarshini Haribaskar [4], Ajith Nagaraj [5], Subbiah Ramasamy [5,*], Priya Rajan [3], Asath Bahadur Sultan [6,*], Mathiyazhagan Ulaganatharaja [1,*]

[1] PG and Research Department of Chemistry, Nadar Mahajana Sangam S.Vellaichamy Nadar (N.M.S.S.V.N.) College, Madurai 625019, Tamil Nadu, India.
[2] Department of Computational Biology, Saveetha School of Engineering, Saveetha Institute of Medical and Technical Sciences (SIMATS), Saveetha University, Chennai 602105, Tamil Nadu, India.
[3] Department of Bioinformatics, School of Life Sciences, Vels Institute of Science Technology and Advanced Studies, Chennai 600117, Tamil Nadu, India.
[4] Center for Bioinformatics, Biomaz Infosearch, Madurai 625706, Tamil Nadu, India.
[5] Department of Biochemistry, School of Biological Sciences, Madurai Kamaraj University, Madurai 625021, Tamil Nadu, India.
[6] Condensed Matter Physics Laboratory, Department of Physics, International Research Center, Kalasalingam Academy of Research and Education, Krishnankoil 626126, Tamil Nadu, India.
* Correspondence: azar2411@gmail.com (A.Z.); s.asathbahadur@gmail.com (A.B.S.); ramasamy.biological@mkuniversity.ac.in (S.R.); svnmur@gmail.com (M.U.)

Scopus Author ID: 57806924200
Received: date; Accepted: date; Published: date

Abstract: This study examines at the molecular interactions of Profenofos with essential human proteins, as well as quantum chemical analysis to optimize its structure and analyze frontier molecular orbitals. The predicted HOMO and LUMO energies were -6.7558 eV and -1.0841 eV, respectively, using DFT-based optimization at the B3LYP/LANL2DZ level. This has resulted in a band gap of 5.6717 eV. Profenofos's persistence in biological and environmental systems is supported by the large energy gap, which shows strong chemical stability and low reactivity. Sirtuin-3 showed the highest binding energy of -6.1 kcal/mol among the protein targets evaluated by molecular docking. This was caused by strong hydrogen bonding, π-alkyl, and electrostatic interactions that promote stable and selective complex formation. Lecithin-Cholesterol Acyltransferase (LCAT), Paraoxonase-1, and Carnitine Palmitoyltransferase-1 (CPT1) showed moderate affinities of -5.4 kcal/mol, -5.8 kcal/mol, and -5.7 kcal/mol, which were mostly maintained by non-polar interactions. With no hydrogen bonding and the weakest interaction (-4.6 kcal/mol), Toll-like Receptor 4 (TLR4) demonstrated poor binding selectivity. High plasma protein binding, low water solubility, and effective intestinal absorption were found by ADMET profiling, indicating restricted free circulation but prolonged retention. Profenofos presents metabolic issues because of cytochrome P450 inhibition and possible endocrine disruption, despite not being mutagenic or cardiotoxic. Furthermore, there are serious threats to ecological systems and human health due to its bioaccumulative nature and environmental toxicity.

Keywords: *Pesticides, Toxicology research, Pharmacokinetics, Diabetes, Molecular docking*

1. Introduction

An essential anabolic hormone, insulin controls the metabolism of fats and carbohydrates. Because of insulin resistance, the metabolic abnormalities linked to diabetes

primarily impact tissues like skeletal muscles, adipose tissue, and the liver [1]. Type 1 diabetes is most frequent in children and teenagers, and it is defined by symptom of substantial hyperglycaemia requiring lifelong insulin therapy. The three main signs of Type 1 diabetes are polydipsia (excessive thirst), polyphagia (increased hunger), and polyuria (frequent urination) [2]. Pancreatic beta cells are destroyed in type 1 diabetes, an autoimmune condition that results in complete insulin insufficiency. Many patients find it difficult to maintain ideal blood glucose control, even though insulin therapy is the standard of care [3]. Insulin resistance is the result of the body's cells not responding appropriately to insulin, which lowers glucose absorption in diabetes people. As a result, blood sugar levels rise, which aids in the development of type 2 diabetes [3]. Patients with type 2 diabetes unable efficiently boost their insulin production to fight insulin resistance because they have a deprived disposition index [1]. High blood sugar, obesity, poor nutrition, inactivity, age, and psychological stress are risk factors. If left unchecked, these variables might lead to problems including persistent hyperglycaemia. Insulin treatment is usually used in conjunction with metformin or other drugs that reduce blood sugar levels [3]. Type 2 diabetes caused the loss of 66.3 million Disability-Adjusted Life Years (DALYs) worldwide in 2019. The burden was corrected for age variations across populations, yielding an age-standardized rate of 801.5 DALYs per 100,000 people. The worldwide health burden from type 2 diabetes since 1990 has increased by 27.6%, demonstrating the disease's increasing prevalence and effect over time [4].

Chemicals called pesticides are used in agriculture to safeguard crops by eliminating or controlling dangerous pests that decrease productivity. They are primarily divided into five categories based on their chemical structure: organochlorines (OCs), organophosphates (OPs), carbamates, pyrethroids, and neonicotinoids. Each category has a distinct toxicity and mechanism of action [5]. The suggested mechanism contains biologically plausible connections between OP (organophosphate) exposure and the development of diabetes, such as oxidative stress, pancreatic β-cell malfunction, and interference with insulin signalling [6]. These chemicals are presented to humans, and because of their hazardous nature, the effects of this exposure on human hormone-dependent diseases are being determined [7]. The organophosphate insecticide profenofos is well-known for its neurotoxic effects and environmental persistence. It affects pests' nervous systems and may cause harm to non-target organisms by inhibiting acetylcholinesterase. Profenofos poses long-term ecological and health problems because of its chemical stability, which causes it to accumulate in soil and water [8]. TLR activation initiates protective inflammation against pathogens and aids tissue repair. However, dysregulated TLR signalling can cause chronic inflammation, leading to autoimmune and inflammatory diseases [9]. TLR-2 and TLR-4 expression and activity in Type 2 diabetes patients' monocytes as well as the enhancing the effects of palmitate, oleate and stearate on the expression of TLR-2 and TLR-4 in high hyperglycaemia [10]. It has been established that the enzyme lecithin acyltransferase (LCAT) may esterify cholesterol in plasma. Human research on the general population and high-risk cardiovascular patients provide misleading results. According to certain research, LCAT activity may encourage atherogenesis. Symptoms of LCAT deficiency include corneal opacities, anaemia, and renal failure, which highlight the pervasive effects of inadequate lipid metabolism [10]. One important enzyme that controls the oxidation of fatty acids (FFAs) is carnitine palmitoyl transferase I (CPT-I), which transforms long-chain fatty acids into a form that can be transported for mitochondrial β-oxidation. Each of its two isoforms: liver and muscle, responds differently to the allosteric inhibitor malonyl-CoA. Malonyl-CoA rises and inhibits CPT-I when insulin levels are high,

which lowers fat oxidation. Malonyl-CoA decreases during fasting, removing the inhibition and enabling the oxidation of FFA and the formation of ketone bodies [11]. The connection between PON1 activity and oxidative stress, finding that elevated oxidative damage was correlated with decreased PON1 activities in T1DM patients [12]. An enzyme called PON-1 aids in the breakdown of dangerous oxidized lipids present in bad cholesterol (LDL), minimizing damage and accumulation. It reduces oxidative stress by acting as a natural antioxidant. Hyperglycaemia, or elevated blood sugar, increases oxidative stress in type 2 diabetes (T2DM) by generating more free radicals [13]. By promoting the PI3K/Akt/mTOR signalling pathway, which increases glucose absorption in adipocytes (fat cells) and aids in the reduction of insulin resistance, Sirt3 activation increases insulin sensitivity [14]. Both type 1 and type 2 diabetes reduce the production of Sirtuin-3 (Sirt3), a key mitochondrial deacetylase enzyme that controls several metabolic processes [15].

These chosen targets are important metabolic pathway regulators linked to diabetes. Carnitine palmitoyl transferase-1 (CPT-1) regulates fatty acid β-oxidation, whereas Sirtuin-3 (SIRT3) controls mitochondrial activity and oxidative stress. Lipid metabolism and antioxidant defense depend on lecithin-cholesterol acyltransferase (LCAT) and paraoxonase-1 (PON1), both of which are frequently compromised in diabetes. Furthermore, inflammatory signaling associated with insulin resistance is mediated by Toll-like receptor 4 (TLR4). These proteins collectively represent interrelated pathways of oxidative stress, inflammation, dyslipidemia, and mitochondrial dysfunction, offering a solid molecular foundation for assessing profenofos's diabetogenic effects [9-15].

Using an *in-silico* molecular docking approach, the current study attempts to assess the molecular interactions and binding affinities of profenofos with important metabolic and regulatory proteins, such as Sirtuin-3, Carnitine palmitoyl transferase-1 (CPT-1), Lecithin-cholesterol acyltransferase (LCAT), Paraoxonase-1 (PON1), and Toll-like receptor 4 (TLR4). The goal of this study is to clarify the possible mechanisms by which exposure to profenofos may lead to the onset of diabetes. By interfering with the normal function of important metabolic and inflammatory proteins, we anticipate that long-term exposure to profenofos, especially through dietary intake, may contribute to the establishment and progression of diabetes. In particular, profenofos may have a strong binding affinity for SIRT3, CPT-1, LCAT, PON1, and TLR4. This could disrupt lipid metabolism, antioxidant defense, mitochondrial function, and inflammatory signaling pathways, which would ultimately result in metabolic dysregulation and diabetes diseases.

2. Materials and Methods

2.1. Retrieval and preparation of protein targets

The protein targets associated with diabetes Sirutuin-3 (PDB ID: 3GLS), Lecithin-cholesterol acyltransferase (PDB ID: 5BV7), Paraoxonase-1 (PDB ID: 1V04), and Toll like receptor-4 (PDB ID: 2Z63) were retrieved from the RCSB Protein Data Bank server [16]. The structure of Carnitine palmitoyl transferase-1 (P50416) was obtained from UniProt database [17]. Before molecular docking, the protein targets were downloaded and refined through the BIOVIA Discovery Studio 2021 client [18]. The pre-processed structural assembly of target proteins were shown in Figure 1. During the pre-processing, the extra residues, ligand structures and water molecules were removed from the target protein's structural assembly. The refined protein structures were saved as pdb format for docking studies.

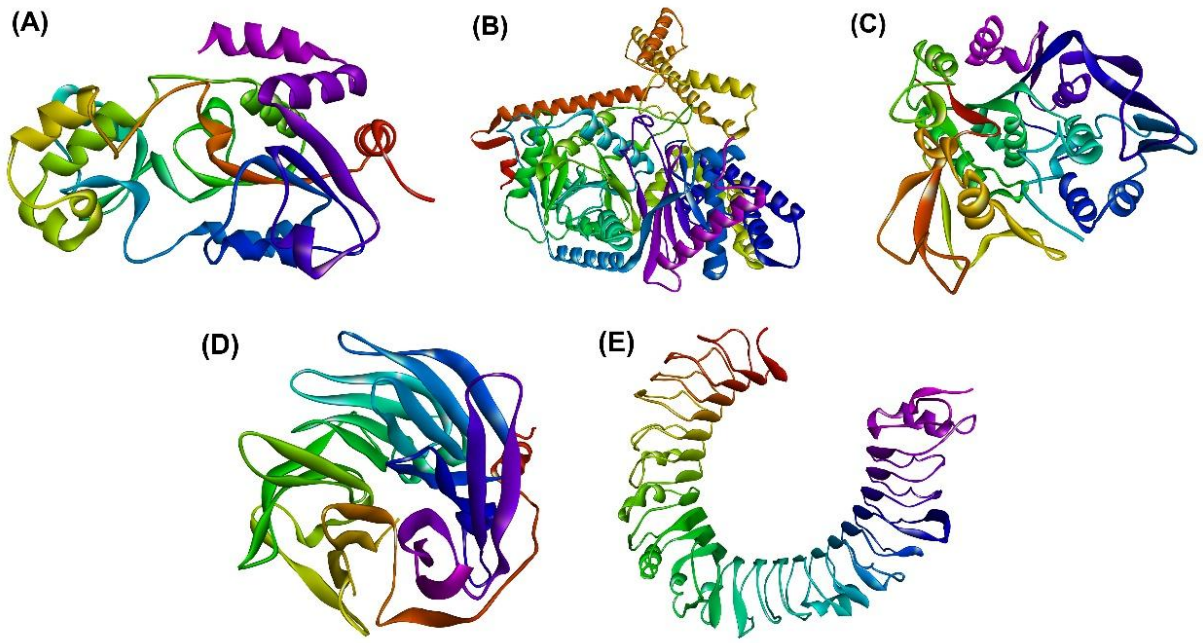

Figure 1. The processed structure of target proteins; **(A)** Sirutuin-3, **(B)** Carnitine palmitoyl transferase-1, **(C)** Lecithin-cholesterol acyltransferase, **(D)** Paraoxonase-1 and **(E)** Toll like receptor 4 using Biovia Discovery studio software.

2.2. Active site prediction

The PrankWeb: Ligand Binding Site Prediction online tool was used to determine the optimal pockets in the active site [19] of targets proteins Sirutuin-3, Carnitine palmitoyl transferase-1, Lecithin-cholesterol acyltransferase and Paraoxonase-1 and for Toll like receptor-4, CASTp online tool was utilized [20]. By utilizing a processed protein structure to query the PrankWeb server, biologically significant annotated residues can be visually observed. The probabilities of the active pockets and the XYZ coordinates of active sites were obtained through this analysis. Further, the ligand will be docked to the target protein's ideal pockets via grid box construction and docking will be performed.

2.3. Ligand retrieval and optimization

The molecular structure of Profenofos, an organophosphorus insecticide, was obtained in the format of "sdf" from the PubChem registry using the CID (38779) [21]. GaussView 5.0 was used to transform the ligand file into a Gaussian input format [22]. Density Functional Theory (DFT) with the B3LYP functional and the LanL2DZ basis set in Gaussian 09W software [23] was used to optimize the structure of the Profenofos molecule. The optimization procedure made sure there were no imaginary frequencies and the molecule was in its lowest energy configuration. The Highest Occupied Molecular Orbital (HOMO) and Lowest Unoccupied Molecular Orbital (LUMO) energies were ascertained using frontier molecular orbital (FMO) analysis after geometry adjustment. To evaluate the stability and chemical response of the profenofos molecule, the energy gap between the HOMO and LUMO was computed. With GaussView, the HOMO-LUMO contour maps were displayed. Further, the virtual and occupied orbitals graphical representation through density of states (DOS) was attained through GaussSum program [24]. These electronic characteristics are critical in future docking studies to understand the ligand's probable interaction with target proteins.

2.4. Molecular docking simulation

Molecular docking is a popular in-silico method used in drug design development. Molecular docking was carried out in this study with PyRx 0.8 software [25]. Initially, the chemical structure of Profenofos was imported in the work space of the PyRx software, followed by the minimization of the energy and conversion into pdbqt format. Pre-processed protein structures were loaded on the graphical window of PyRx and was assigned as macromolecules. Further, in the control window, the processed ligand and protein structures were selected in the Vina wizard panel. Then, the grid was build based on the X, Y and Z co-ordinates assessed from Active site prediction. Docking was performed. Nine different poses of ligand binding were performed for every run and the results were generated with the RMSD values of upper bound and lower bound. The docking scores were selected based on the lowest RMSD values among nine poses. The results were saved as "pdbqt" output file and the scores were stored in "csv" format.

2.5. Analysis of protein-ligand interaction

BIOVIA Discovery Studio Visualizer [18] was used to assess the ligand-protein interaction based on the docking output in "pdbqt" format. To observe the binding orientation and interaction patterns between the proteins and profenofos, the complex was imported. To determine the significant residues involved in binding, two-dimensional interaction images were created. Hydrophobic contacts and hydrogen bonds were among the types of interactions that were described, along with the corresponding bond lengths. The bond distances between the ligand and key amino acid residues were measured to assess the strength and stability of the interactions. This analysis provided insight into the binding affinity and specificity of the profenofos towards the target proteins. The detailed interaction profile was used to support the docking scores and evaluate the profenofos therapeutic potential.

2.6. Analysis of ADMET profile

SwissADME and pKCSM online prediction programs were used to assess the Profenofos ligand's ADMET and pharmacokinetic characteristics [26, 27]. Both platforms used the optimized Profenofos structure's SMILES notation as input. Physicochemical characteristics, lipophilicity, water solubility, and drug-likeness were evaluated using SwissADME in accordance with Lipinski's rule. The absorption, distribution, metabolism, excretion, and toxicity (ADMET) profiles were predicted by the pKCSM program. Important factors were examined, including hepatotoxicity, cytochrome P450 inhibition, intestinal absorption, and blood-brain barrier permeability. These forecasts provide information about Profenofos safety profile and drug-likeness for possible medical uses.

3. Results

3.1. Analysis of Active sites

In the present study, active site residues of five target proteins Sirtuin-3, Carnitine Palmitoyl Transferase-1 (CPT-1), Lecithin-Cholesterol Acyltransferase (LCAT), Paraoxonase-1, and Toll-Like Receptor 4 (TLR4) were analyzed to elucidate the potential binding sites that mediate ligand interface and functional modulation. The predicted active site regions were represented in Figure 2. The target Sirtuin-3 exhibited a total of 38 key residues, that were

predicted to be D_145, D_146, D_147, D_149, D_150, D_154, D_155, D_156, D_157, D_158, D_177, D_180, D_195, D_199, D_228, D_229, D_230, D_231, D_248, D_291, D_292, D_293, D_294, D_295, D_296, D_298, D_319, D_320, D_321, D_322, D_323, D_324, D_325, D_344, D_345, D_346, D_348, D_366 with a score of 40.32 and a probability of 0.959, indicating robust poise in the active site prediction. In CPT-1, a total of 42 active residues: A_236, A_239, A_240, A_241, A_250, A_251, A_252, A_254, A_295, A_296, A_297, A_303, A_473, A_477, A_478, A_479, A_589, A_591, A_592, A_593, A_595, A_602, A_644, A_654, A_655, A_658, A_661, A_662, A_678, A_680, A_682, A_685, A_686, A_687, A_688, A_689, A_690, A_711, A_712, A_713, A_715, A_723 were identified, with a score of 35.37 and a prediction confidence of 0.943. These residues are scattered across a large binding boundary, signifying flexibility and adaptableness in substrate accommodation. For the target LCAT, 24 key residues were mapped with a modest score of 14.61 and a probability of 0.738. The mapped ideal pockets were A_120, A_180, A_181, A_182, A_212, A_216, A_218, A_219, A_222, A_223, A_232, A_233, A_234, A_248, A_249, A_252, A_253, A_30, A_31, A_32, A_347, A_348, A_377, A_378, respectively. The relatively lower score depicts a smaller and possibly more selective binding areas of LCAT structure.

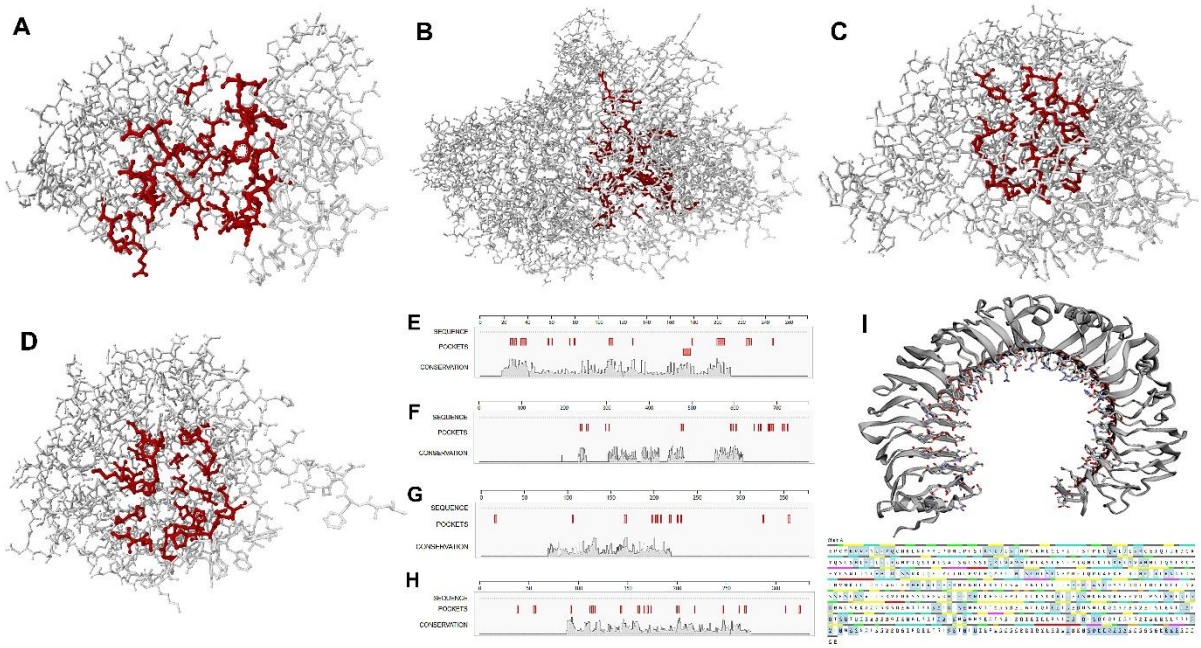

Figure 2. Predicted ideal active pockets of the proteins with their sequences **(A, E)** Sirutuin-3, **(B, F)** Carnitine palmitoyl transferase-1, **(C, G)** Lecithin-cholesterol acyltransferase, **(D, H)** Paraoxonase-1 using PrankWeb tool and **(I)** Toll like receptor 4 via CASTp tool.

Paraoxonase-1 exhibited a total of 27 key amino residues with a score of 21.76 and a probability confidence of 0.856. The 27 key residues of Paraoxonase-1 were A_115, A_134, A_136, A_137, A_139, A_165, A_166, A_183, A_184, A_189, A_192, A_193, A_196, A_222, A_224, A_240, A_269, A_285, A_291, A_292, A_332, A_346, A_347, A_53, A_69, A_70, A_71, respectively. The target TLR4 active site was the most widespread, with over 100 amino residues. The massiveness of this active site correlates with its role in recognizing a wide array of pathogen-associated molecular patterns (PAMPs). The predicted active residues of TLR4 were A_31, A_32, A_33, A_34, A_36, A_37, A_38, A_39, A_57, A_58, A_59, A_60, A_62, A_63, A_81, A_82, A_84, A_86, A_87, A_103, A_105, A_106, A_108, A_110, A_129, A_130, A_132, A_134, A_135, A_153, A_154, A_156, A_158, A_159, A_178, A_179,

A_181, A_183, A_184, A_205, A_207, A_208, A_209, A_211, A_212, A_229, A_230, A_232, A_234, A_235, A_256, A_257, A_259, A_261, A_263, A_287, A_289, A_291, A_293, A_312, A_314, A_316, A_317, A_334, A_336, A_338, A_339, A_355, A_357, A_359, A_360, A_376, A_377, A_379, A_381, A_382, A_402, A_403, A_405, A_407, A_408, A_425, A_426, A_428, A_430, A_450, A_451, A_453, A_455, A_456, A_474, A_475, A_477, A_479, A_499, A_500, A_502, A_504, A_505, A_523, A_524, A_526, A_528, A_529, A_547, A_548, A_550, A_552, A_570, A_574, A_575, A_576, A_577, A_578, A_579, A_580, A_581, A_589, A_590, A_591, respectively. The predicted active site residues effectively guided the grid construction zone in molecular docking studies and offered mechanistic insights into ligand binding. These findings pave the way for further validations on therapeutic targeting of key metabolic and signaling proteins [28-30].

3.2. Ligand optimization and FMO analysis

The optimization of Profenofos using Gaussian 09w with the B3LYP/LANL2DZ basis set revealed a stable geometry [31]. The results of Frontier Molecular Orbital (FMO) mapped surfaces and Density of States (DOS) were represented in Figure 3. The FMO analysis showing a HOMO energy of -6.7558 eV and a LUMO energy of -1.0841 eV, yielding a significant band energy gap of 5.6717 eV.

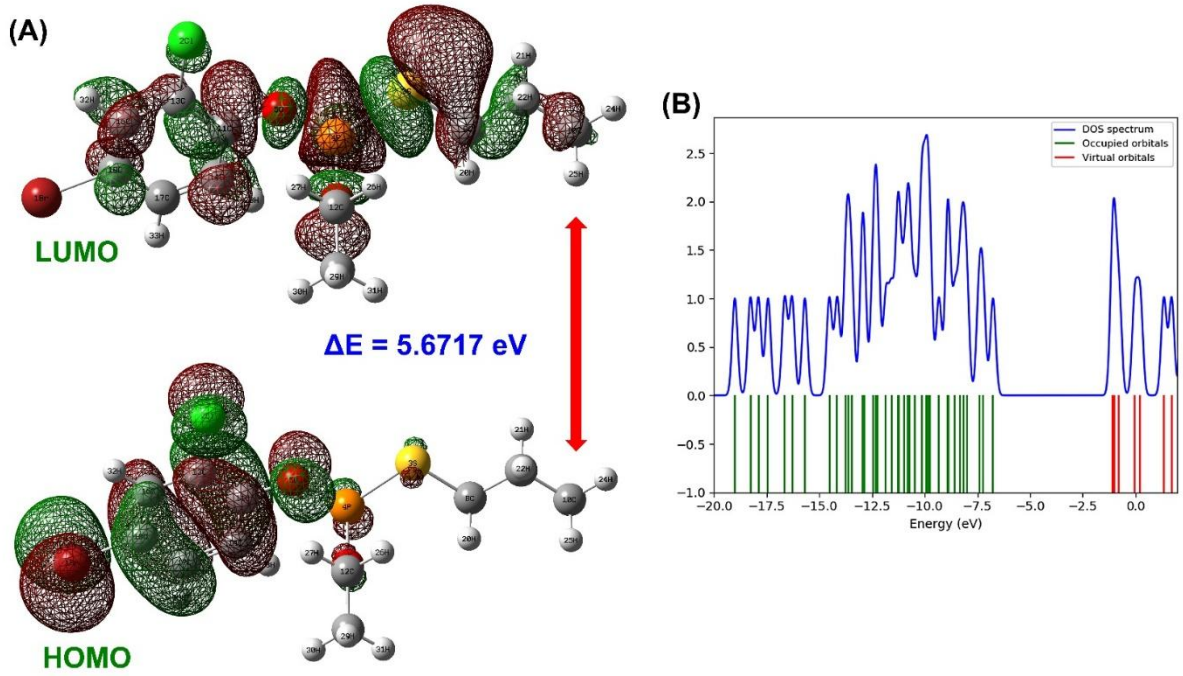

Figure 3. Generated orbital maps of LUMO and HOMO of optimized Profenofos structure **(A)** and the simulated Density of States (DOS) spectrum illustrating occupied orbitals and virtual orbitals in green and red colors **(B).**

This larger HOMO-LUMO gap indicates high chemical stability, signifying selective binding behaviour. Such stability is beneficial from a biological perspective because it enables the ligand to preserve its structural integrity in the dynamic environment of the protein binding site, promoting consistent interaction patterns.The spectrum demonstrated a clear distribution of molecular orbitals, with HOMO orbitals predominantly localized around electronegative atoms, potentially serving as electron donors in interaction scenarios. The LUMO orbitals, localized near electrophilic regions, recommend latent sites for nucleophilic attack or hydrogen

bonding with target proteins. The possibility of particular interactions with amino acid residues is increased by this spatial separation of border orbitals, especially through charge transfer and hydrogen bonding mechanisms. These FMO values highlight the role of orbital symmetry and electronic density in ligand-protein interactions. The deep HOMO energy recommends limited electron donation ability, preventing non-specific interactions and favouring targeted binding. Strong binding is made possible by the molecule's stability and electrical structure without losing receptor integrity [32-35]. The bioactive conformation is kept constant during the docking process by the large band gap, which also lessens the possibility of spontaneous electron transitions. In order to achieve stable and repeatable docking interactions, this guarantees that the ligand maintains its optimal shape upon binding. Overall, the DOS profile and optimized structure confirm that Profenofos is an electrically selective, chemically stable molecule with advantageous characteristics for interacting with biological macromolecules, , thereby supporting its potential role in modulating target protein activity at the molecular level.

3.3. Molecular docking simulation

The pesticide Profenofos interacts with target proteins, exhibiting different levels of hydrogen bonding and binding affinity, according to the molecular docking studies [36, 37]. The results of molecular docking studies were shown in Table 1 and Figure 4. With the greatest binding affinity of -6.1 kcal/mol among the studied proteins, Sirtuin-3 formed two conventional hydrogen bonds, indicating a persistent and particular interaction that may be biologically relevant in controlling metabolism and oxidative stress. Additionally, Paraoxonase-1 established three hydrogen bonds and had a favorable binding affinity of -5.7 kcal/mol, suggesting a potentially powerful and precise interaction with the ligand. Toll-like receptor 4, LCAT, and CPT-1 on the other hand, did not form any conventional hydrogen bonds and displayed weaker to moderate binding affinities ranging from -4.6 to -5.8 kcal/mol.

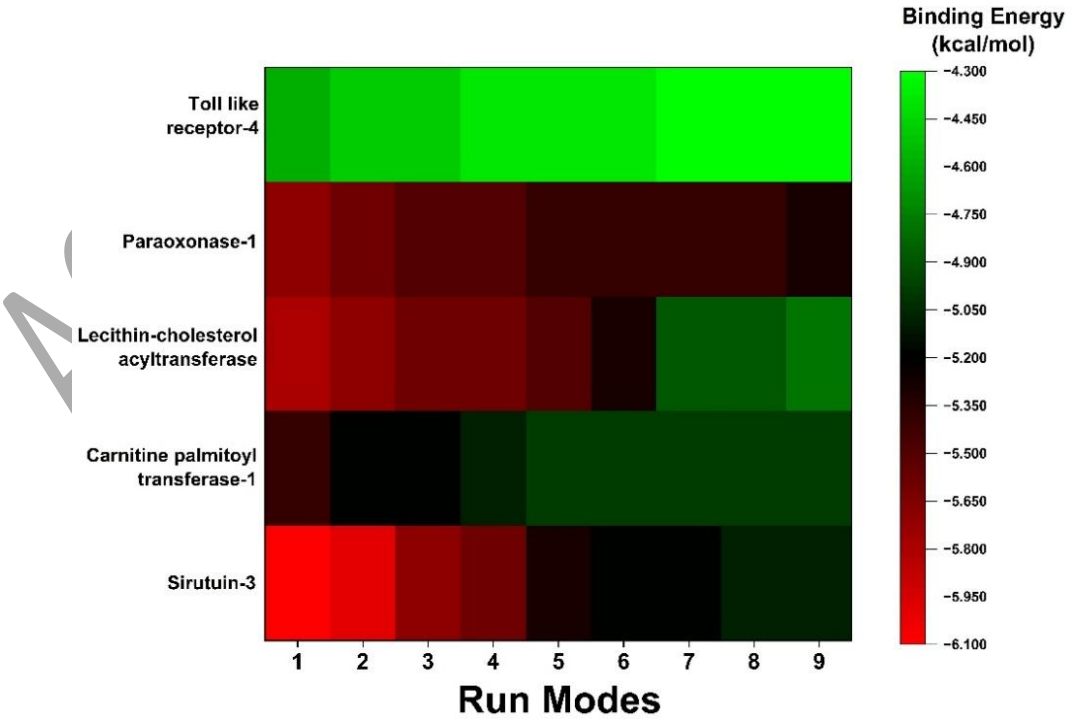

Figure 4. Heatmap illustration of binding energies of target proteins at different run modes when docked with organophosphate pesticide Profenofos through Molecular docking analysis.

With RMSD lower bound (LB) and upper bound (UB) values of 0.0 Å, the top-ranked pose (Mode 1) is the reference conformation with the best stable binding orientation. The other docking positions (Modes 2–9), on the other hand, showed a broad RMSD distribution that ranged from roughly 2.0 to 49.0 Å in relation to the optimal stance. Moderate conformational variations are indicated by RMSD values between 2.0 and ~5.0 Å, indicating partially comparable binding orientations that might yet preserve important interactions within the active site. However, significant structural divergence is indicated by RMSD values that go much beyond this range (especially >10 Å and up to ~49.0 Å). This fluctuation may be seen as a sign of the flexibility of the ligand's structure and its capacity to adjust to various areas of the protein environment. The RMSD distribution confirms the presence of several energetically viable orientations together with a dominant and stable binding mode. This adaptability increases the ligand's possible biological significance by demonstrating its capacity to sustain connections across a range of conformational circumstances. With the top-ranked pose acting as the most likely binding conformation for additional examination and validation, the docking data can therefore be regarded as trustworthy. This recommends that their interactions may be less specific or primarily driven by van der Waals or hydrophobic forces. All things considered, Profenofos exhibited a potent binding with the target Sirutuin-3 associated to diabetes.

Table 1. Calculated binding energies of Target proteins when docked with Profenofos along with their Root mean square deviation (RMSD) values at different run modes.

Proteins	Binding Energy (kcal/mol)	RMSD (U.B.)	RMSD (L.B.)
Sirutuin-3	-6.1	0	0
	-6	47.273	45.003
	-5.7	46.109	43.454
	-5.6	4.749	3.261
	-5.3	45.665	43.006
	-5.2	39.016	37.486
	-5.2	40.965	38.818
	-5.1	39.033	37.896
	-5.1	60.039	58.218
Carnitine palmitoyl transferase-1 (CPT1)	-5.4	0	0
	-5.2	2.826	2.285
	-5.2	44.798	42.746
	-5.1	44.701	42.617
	-5	6.6	3.944
	-5	44.283	42.211
	-5	43.987	41.888
	-5	45.169	43.237
	-5	45.458	43.509
Lecithin-cholesterol acyltransferase (LCAT)	-5.8	0	0
	-5.7	23.334	21.329
	-5.6	23.72	21.754
	-5.6	23.468	21.596
	-5.5	22.738	20.9
	-5.3	19.931	19.1
	-4.9	19.971	18.943
	-4.9	23.645	21.379
	-4.8	24.132	22.266

Paraoxonase-1	-5.7	0	0
	-5.6	5.824	3.573
	-5.5	4.521	3.05
	-5.5	5.814	3.477
	-5.4	5.848	3.582
	-5.4	5.839	4.098
	-5.4	24.357	22.564
	-5.4	3.928	2.727
	-5.3	5.274	3.733
Toll like receptor 4 (TLR4)	-4.6	0	0
	-4.5	23.929	22.722
	-4.5	5.858	3.611
	-4.4	5.574	3.708
	-4.4	39.322	37.586
	-4.4	5.73	4.058
	-4.3	6.637	3.852
	-4.3	3.696	2.887
	-4.3	49.312	47.759

3.4. Interaction of Protein-Ligand

The interactions formed between the pesticide Profenofos and the target proteins were analysed through Discovery studio tool. The binded poses and interacted 2D, 3D interactions were shown in Figure 5, Figure 6 and Figure 7. The docking studies of profenofos with the target protein demonstrated a stable binding conformation inside the active region. Important interactions between the ligand and the amino acid residues His426, Lys402, and Ile450 were observed. Profenofos specifically established alkyl and π-alkyl connections with these residues, suggesting that the ligand is primarily stabilized inside the binding pocket. Possessing bromine and chlorine substituents, the aromatic ether ring of profenofos was found close to Ile450 and His426, indicating the potential for advantageous π-alkyl stacking interactions. The TLR4 protein and profenofos showed a persistent binding inside the active region, mostly due to hydrophobic interactions, and established a π-alkyl contact with His426 (5.38 Å) and alkyl connections with Lys402 (4.90 Å) and Ile450 (4.75 Å). The bromine-containing aromatic ether ring was found close to Ile450 and His426, indicating potential π-stacking or halogen interactions. The profenofos is adequately accommodated in the binding pocket through hydrophobic contacts with the LCAT protein through alkyl, π-alkyl, and π-sigma interactions with amino residues Lys218, Pro219, Val222, Ile233, Pro232, Pro250, and Phe253 and these interactions, range from 3.9 to 5.1 Å distances, imply that van der Waals and hydrophobic forces are the main stabilizing factors. Multiple hydrophobic interactions resulted in persistent binding between profenofos and Carnitine Palmitoyl transferase 1 (CPT1), with Tyr220, Tyr666, and Trp227 through π-alkyl connections, whereas Ala228, Val663, Leu223, Leu667, and Lys224 established alkyl contacts and a single π-sigma interaction with Tyr666 was observed with a bond distance range of 3.66–5.49 Å. When profenofos and paraoxonase-1 were docked, a stable binding posture was supported by both hydrophobic and hydrogen bonding interactions, such as carbon hydrogen bonds with Asp269, conventional hydrogen bonds with Asn168 and His115 and hydrophobic interactions with Leu69, His134, and Phe292, including alkyl and π-alkyl contacts.

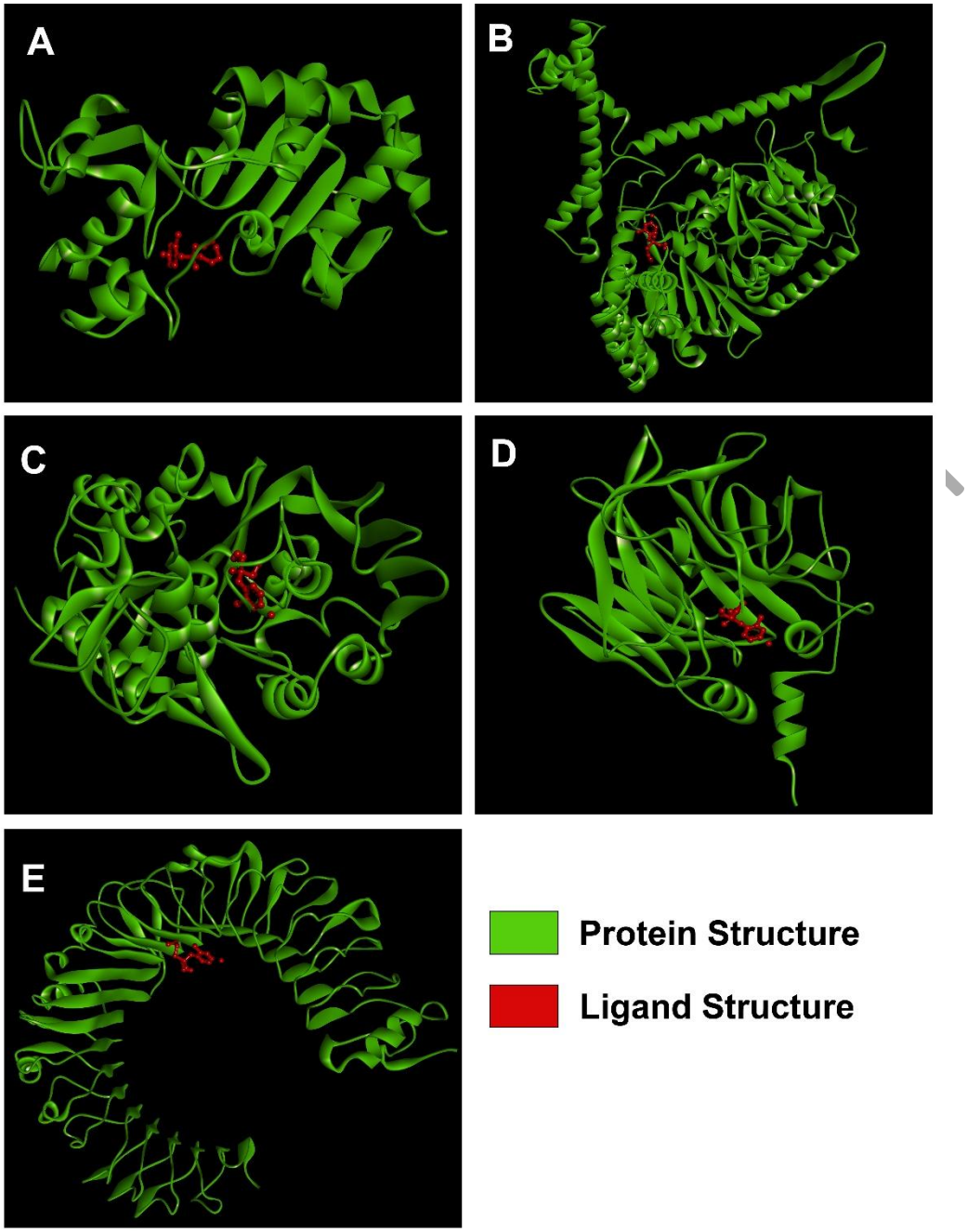

Figure 5. Docked poses of Profenofos with the target proteins **(A)** Sirutuin-3, **(B)** Carnitine palmitoyl transferase-1, **(C)** Lecithin-cholesterol acyltransferase, **(D)** Paraoxonase-1 and **(E)** Toll like receptor 4 visualized through Discovery studio software.

The hydrogen bonds were found with distances ranging from 2.27 to 3.78 Å, demonstrating stable and targeted interactions and the hydrophobic contacts were also found in distance from 4.3 to 5.1 Å, respectively. With a higher docking score of -6.1 kcal/mol, profenofos binds to the Sirtuin-3 active site firmly, suggesting a positive interaction. The ligand forms two conventional hydrogen bonds with Arg158, at distances of 2.82 Å and 2.31 Å respectively, which play a crucial role in stabilizing the protein-ligand complex. The profenofos with His248 exhibited an electrostatic pi-cation interaction, improving binding selectivity. Significant contributions to ligand stabilization are also made via hydrophobic contacts with amino residues Val324 (alkyl interaction), Phe180 (pi–pi stacking), Phe180, Phe294, and His248 (pi–alkyl interactions), respectively. The strong binding of profenofos within the Sirtuin-3 pocket is supported by these interactions, which range in distance from 3.7

Å to 5.1 Å [38, 39]. Altogether, this interaction profile points to the possibility that profenofos may alter Sirtuin-3 activity, which might have an effect on metabolic control, oxidative stress response, and mitochondrial function in diabetes situations.

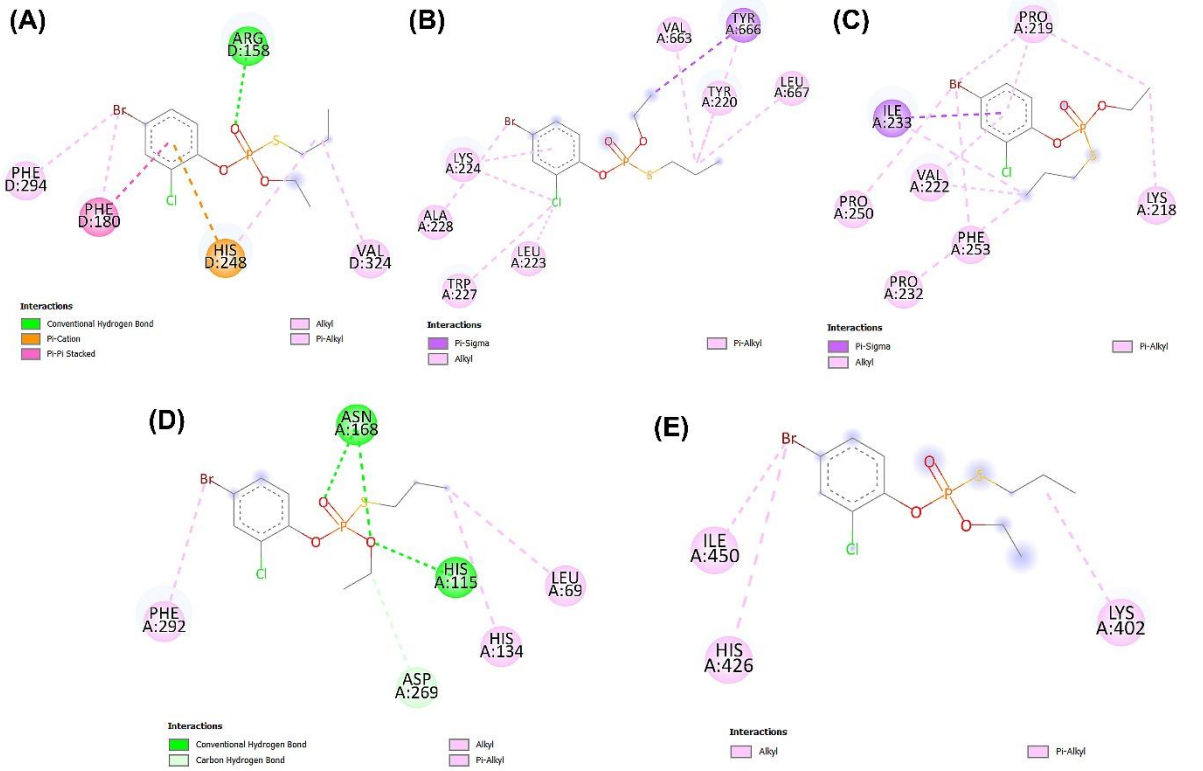

Figure 6. Pictorial representation of two-dimensional interactions of Profenofos with target proteins **(A)** Sirutuin-3, **(B)** Carnitine palmitoyl transferase-1, **(C)** Lecithin-cholesterol acyltransferase, **(D)** Paraoxonase-1 and **(E)** Toll like receptor 4 with bond types.

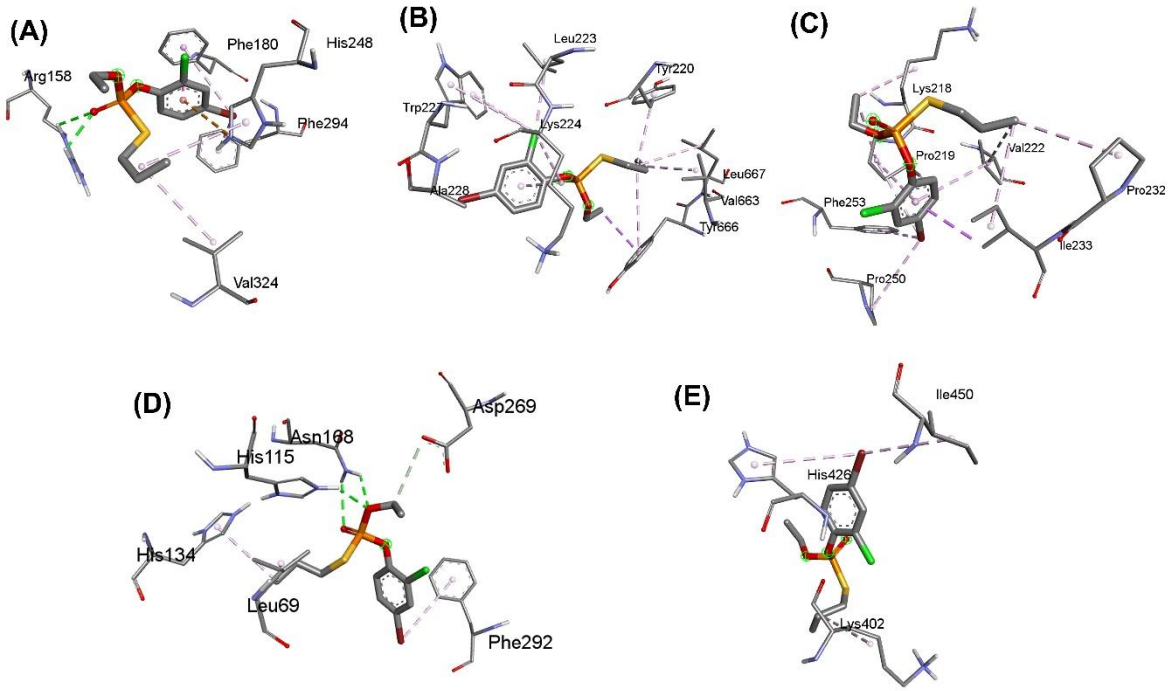

Figure 7. Pictorial representation of three-dimensional interactions of Profenofos with target proteins **(A)** Sirutuin-3, **(B)** Carnitine palmitoyl transferase-1, **(C)** Lecithin-cholesterol acyltransferase, **(D)** Paraoxonase-1 and **(E)** Toll like receptor 4 with bond types.

3.5. SwissADME analysis

Profenofos is an organophosphate insecticide with the molecular formula $C_{11}H_{15}BrClO_3PS$ and a molecular weight of 373.63 g/mol, was investigated for ADME analysis using SwissADME server. An *in-silico* analysis reveals that it has moderate water solubility and high gastrointestinal absorption, suggesting efficient uptake in biological systems. However, it is not permeable to the blood-brain barrier and is not a P-glycoprotein substrate. Profenofos inhibits multiple cytochrome P450 enzymes (CYP1A2, CYP2C19, CYP2C9), indicating a strong potential for metabolic disruption and drug-enzyme interactions. The generated Boiled-Egg plot was generated and the result was shown in Figure 8. From, the Boiled-Egg plot profenofos was shown a higher Human Intestinal Absorption (HIA), which is a critical factor in its toxicokinetic profile. Elevated HIA recommends that upon exposure particularly through ingestion it can readily enter systemic circulation, increasing the potential for toxic effects in humans. This high rate of absorption and its strong binding to plasma proteins suggest that even while it circulates in a bound state, it stays in the body for extended periods of time, which may result in bioaccumulation. The danger of chronic toxicity is increased by such persistence, particularly when exposure occurs often or over an extended period of time [40]. The profenofos synthetic accessibility score of 4.21 and the absence of PAINS alerts suggest as a tractable molecule for further toxicological evaluation. Furthermore, Profenofos is predicted to block cytochrome P450 enzymes, which might exacerbate the toxic load by interfering with regular metabolic detoxification processes. Another reason for caution is raised by the possibility that it may interfere with endocrine signaling, especially in susceptible groups like pregnant women and children [41]. Because of these characteristics, profenofos presents serious toxicological hazards when taken orally, necessitating strict control and close observation. Food or water sources contaminated by the environment aggravate these health issues for people.

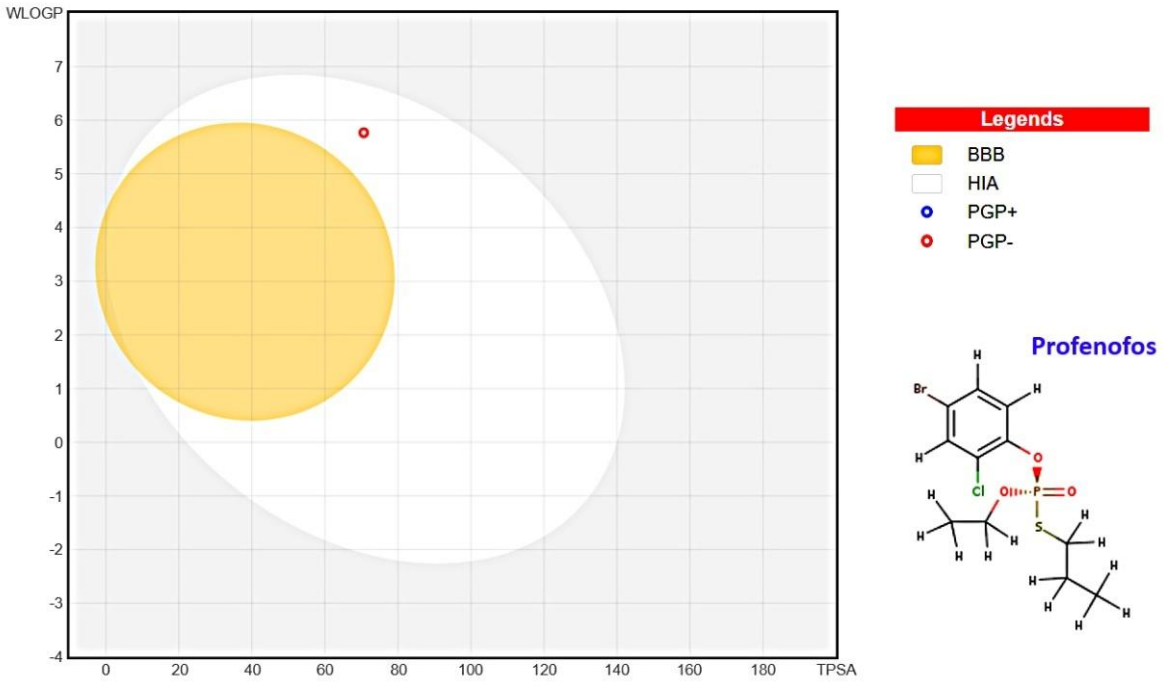

Figure 8. Generated Boiled-Egg model for Profenofos structure in SwissADME tool. The pesticidal compound profenofos has showed better Human Intestinal Absorption (HIA) by presenting in the white zone of Boiled-Egg map as a P-glycoprotein negative molecule.

3.6. Pharmacokinetic studies

The pharmacokinetic parameters of the organophosphate pesticide Profenofos were analysed through pkCSM tool and the results were tabulated in Table 2. The pharmacokinetic profiling of profenofos, performed using the pkCSM tool, provides significant insight into its absorption, distribution, metabolism, and toxicity (ADMET) behaviour [42]. The compound demonstrates high human intestinal absorption (87.1%) and moderate Caco-2 permeability (1.839 log Papp), which together suggest favorable oral bioavailability. However, its poor aqueous solubility (log S = -5.719) could hinder dissolution and absorption under certain conditions. Low skin permeability (log Kp = -2.856) indicates that dermal exposure is unlikely to be a major route of toxicity. The absence of interaction with P-glycoprotein transporters minimizes the risk of efflux-mediated absorption loss. In terms of systemic distribution, profenofos exhibits moderate volume of distribution and high plasma protein binding, suggesting limited free drug concentration in plasma but potentially extended retention within the body. The profenofos's ability to moderately cross the blood-brain barrier (log BB = 0.321) but with poor CNS permeability (log PS = -2.337) implies minimal central nervous system accumulation. Metabolically, profenofos is a substrate of CYP3A4 and an inhibitor of CYP1A2 and CYP2C19, indicating it could interfere with hepatic metabolism and potentially disrupt endocrine pathways. Its lack of interaction with other major CYP enzymes such as CYP2D6, CYP2C9, and CYP3A4 (as an inhibitor) reduces the likelihood of widespread metabolic drug-drug interactions. Toxicity predictions are concerning, with potential for chronic effects at low exposure levels (LOAEL = 0.705 log mg/kg/day), even though it is non-mutagenic, non-hepatotoxic, and non-cardiotoxic by *in-silico* screening. Moreover, the moderate clearance rate and absence of OCT2-mediated renal elimination, combined with high lipophilicity and protein binding, point toward a tendency for bioaccumulation. Notably, environmental toxicity toward aquatic species further emphasizes the persistent and hazardous nature of profenofos [43]. Taken together, the predicted ADMET profile suggests that chronic low-dose exposure may not only lead to bioaccumulation but also potentially contribute to metabolic dysregulation, including insulin resistance and type 2 diabetes, especially considering its hepatic enzyme inhibition profile. Overall, this computational study provides a foundational framework for understanding the pharmacological and toxicological behaviour of profenofos, highlighting its potential role in metabolic disruption, environmental toxicity, and public health risk.

Table 2. The predicted results of ADMET parameters of pesticide Profenofos using pKCSM tool.

Property	Model Name	Predicted Value
Absorption	Water solubility (log mol/L)	-5.719
	Caco2 permeability (log Papp in 10^{-6} cm/s)	1.839
	Human Intestinal absorption (%)	87.115
	Skin Permeability (log Kp)	-2.856
	P-glycoprotein substrate	No
	P-glycoprotein I inhibitor	No
	P-glycoprotein II inhibitor	No
Distribution	Human VDss (log L/kg)	-0.009
	Human Fraction unbound (Fu)	0.069
	BBB permeability (log BB)	0.321
	CNS permeability (log PS)	-2.337
Metabolism	CYP2D6 substrate	No

	CYP3A4 substrate	Yes
	CYP1A2 inhibitior	Yes
	CYP2C19 inhibitior	Yes
	CYP2C9 inhibitior	No
	CYP2D6 inhibitior	No
	CYP3A4 inhibitior	No
Excretion	Total Clearance (log ml/min/kg)	0.145
	Renal OCT2 substrate	No
Toxicity	AMES toxicity	No
	Max. tolerated dose (human) (log mg/kg/day)	1.137
	hERG I inhibitor	No
	hERG II inhibitor	No
	Oral Rat Acute Toxicity (LD50) (mol/kg)	3.698
	Oral Rat Chronic Toxicity (LOAEL) (log mg/kg_bw/day)	0.705
	Hepatotoxicity	No
	Skin Sensitisation	No
	T. Pyriformis toxicity (log ug/L)	1.448
	Minnow toxicity (log mM)	-0.991

3.7. Impact of Profenofos on molecular targets associated to Diabetes

The interaction of profenofos, an organophosphate pesticide, with key regulatory proteins involved in metabolic homeostasis may significantly influence the pathophysiology of diabetes and its associated complications (Figure 9).

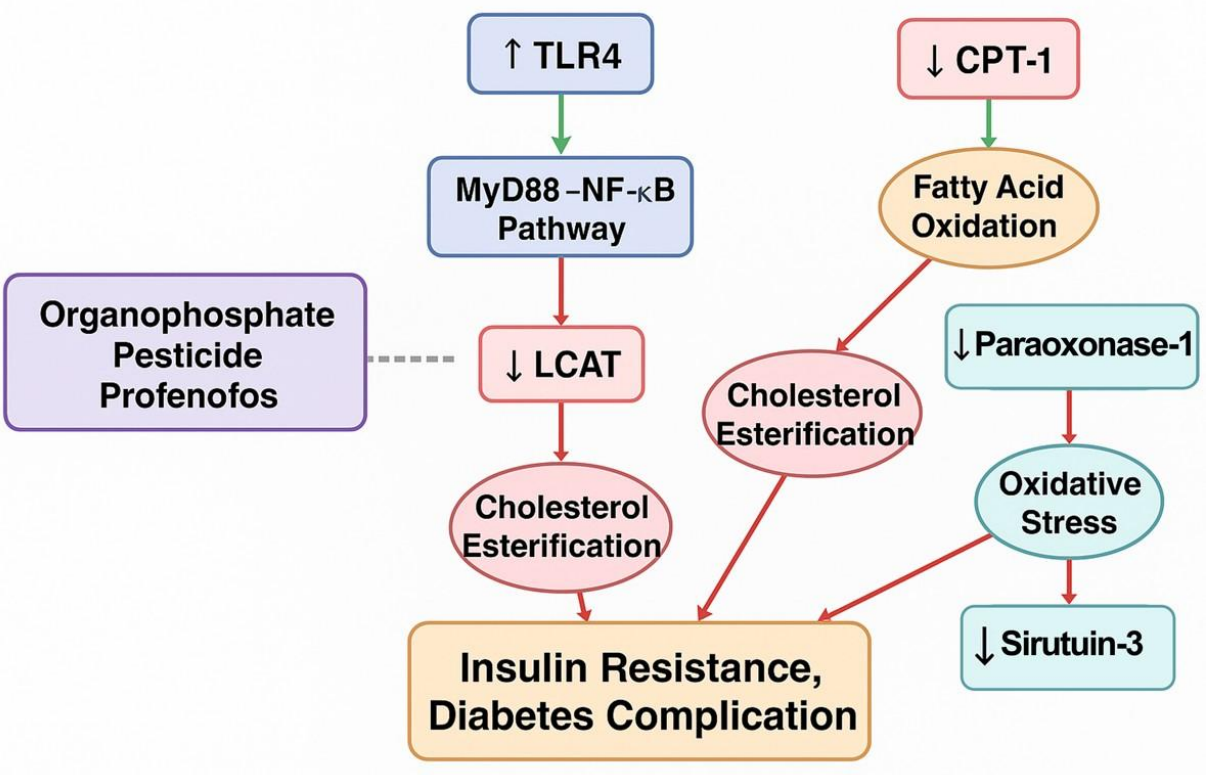

Figure 9. Graphical representation of Molecular interactions pathway of target proteins associated with Diabetes and the impact of Profenofos in these pathways.

The computational analyses suggest that profenofos may interfere with Toll-like receptor 4 (TLR4), a major proinflammatory receptor. Profenofos exposure is linked to oxidative stress and immunotoxicity, which could potentiate TLR4 expression and activation. This leads to the stimulation of the MyD88–NF-κB pathway, resulting in elevated production of proinflammatory cytokines such as IL-6 and TNF-α. Such chronic inflammation is a recognized driver of insulin resistance and β-cell dysfunction, thereby accelerating the onset of type 2 diabetes [44]. Profenofos might alter lipid homeostasis by modulating lecithin–cholesterol acyltransferase (LCAT) function. The lipophilic nature and high bioaccumulation potential can disturb lipid signaling, potentially impairing LCAT activity and reverse cholesterol transport [10]. The profenofos's influence on carnitine palmitoyltransferase-1 (CPT-1) is also critical and may induce metabolic stress may upregulate CPT-1 expression as a compensatory mechanism to favour fatty acid oxidation [11]. However, chronic overexpression of CPT-1 leads to energy imbalance in peripheral tissues, aggravating insulin resistance and impairing glucose utilization. Moreover, aggravation of profenofos may lead to the reduced activity of Paraoxonase-1 in diabetic condition [12]. The top hit target Sirutuin-3, a mitochondrial deacetylase involved in maintaining redox balance and metabolic flexibility, may be negatively affected by profenofos exposure [14]. By inducing mitochondrial stress and ROS accumulation, profenofos may suppress Sirutuin-3 activity, thereby impairing fat metabolism, insulin signaling, and cellular stress responses [14]. Collectively, these findings highlight that profenofos can dysregulate multiple molecular targets central to metabolic and inflammatory pathways. Its chronic exposure may exacerbate metabolic disorders, promote insulin resistance, and increase the risk of diabetes-related complications, suggesting an urgent need to assess such pesticides for their endocrine-disrupting and diabetogenic potential.

4. Discussion

The current study aims to offer a computational account of the electronic properties, binding, and pharmacokinetic behavior of profenofos, with special emphasis on its possible interaction with protein targets related to metabolic control. From the Density Functional Theory (DFT) computations, a large HOMO-LUMO gap was calculated, implying that profenofos has considerable stability and a lower reactivity. From a biological point of view, this stability could be related to the maintenance of the ligand's conformation in protein-binding pockets, thus allowing for reproducibility of interaction patterns. It is, however, necessary to exercise caution in the interpretation of these results, since stability in terms of electronic behavior does not necessarily translate to efficacy or toxicity in a biological system. The spatial distribution of frontier orbitals revealed that there are areas in the profenofos molecule that could be related to electron donation and acceptance, thus allowing for non-covalent interactions, including those related to hydrogen bonding and charge transfer, particularly with amino acid residues. These are usually related to protein-ligand recognition, although it is necessary to exercise caution in this respect since this is dependent on a variety of factors related to the cellular environment, which is usually not taken into account in computational models. From this analysis, it is clear that profenofos has the ability to interact with various target proteins, such as Sirtuin-3 and Paraoxonase-1, with moderate binding affinity. The presence of hydrogen bonds in some complexes indicates specific interactions, which might be responsible for altering the functions of these proteins. The interaction with Sirtuin-3, which is responsible for mitochondrial metabolism and oxidative stress, indicates a possible pathway

for profenofos in altering metabolic pathways. The binding energy for each protein is in the moderate range. The docking results do not confirm biological activities; they only predict them. The results from RMSD analysis indicate the presence of one major binding conformation with low energy, along with several alternative conformations. This indicates that profenofos has conformational flexibility. The results from docking analysis, therefore, confirm that profenofos has the ability to adapt to various binding conditions. The results from ADMET prediction, which were generated using the pkCSM tool, also provide further insight into how profenofos behaves in a biological system. The results from ADMET prediction confirm that profenofos has high intestinal absorption and moderate permeability. The results also confirm that profenofos is likely to be absorbed quickly upon exposure. The lipophilicity and plasma protein binding capacity of profenofos confirm its ability to be retained in the body. The interaction with specific cytochrome P450 enzymes such as CYP3A4, CYP1A2, and CYP2C19 indicates profenofos's ability to interfere with metabolic pathways. Although the absence of acute mutagenic and organ toxicity is recommended by the predictions, the implications for chronic effects and persistence in the environment should not be dismissed. The possibility of bioaccumulation, as suggested by the lipophilicity and clearance parameters, could lead to chronic biological effects. However, it is noteworthy that the association between profenofos exposure and metabolic disorders, such as insulin resistance or diabetes, is hypothetical in nature, relying solely on the computation of associations with relevant protein targets. Overall, this study demonstrates the potential interaction of profenofos with biologically relevant macromolecules and pharmacokinetic profiles that are suggestive of systemic exposure. However, all these findings are based on computational models and should be considered preliminary. Predictive models used in computational toxicology research may not adequately represent the intricacy of biological systems, including elements like metabolism, protein dynamics, and cellular context. The quality of the input data and algorithms, which may create bias or uncertainty, also affects the accuracy of the outputs. It is important to validate these interactions through experimental approaches like in vitro and in vivo studies to confirm these interactions and establish any possible relationship between profenofos exposure and metabolic outcomes.

5. Conclusion

By combining molecular docking and quantum chemistry studies, this study offers a computational understanding of the possible toxicity profile of profenofos. While lesser interactions with TLR4 indicate poor target selectivity, the chemical showed moderate binding interactions with important metabolic proteins, especially Sirtuin-3 and Paraoxonase-1. High chemical stability is indicated by its electrical characteristics, which could support environmental persistence and potential bioaccumulation. Along with drawbacks including poor solubility and possible interference with cytochrome P450 enzymes, pharmacokinetic projections also point to robust plasma protein binding and favorable absorption. These results are based only on in-silico models, but they suggest potential metabolic and toxicological implications. In order to validate these hypotheses and gain a better understanding of the biological effects of profenofos in the real world, experimental validation is required.

Conflicts of Interest

The authors have no relevant financial or non-financial interests to disclose.

Ethical approval and consent to participate

This article does not contain any studies with human or animal subjects performed by any of the authors.

Acknowledgments

The authors are grateful to the Biomaz Infosearch, Madurai, Tamil Nadu, India for the technical support and research facilities.

Author Contribution

Conceptualization: A.Z., M.U. and M.M.; Methodology: M.M., A.Z., N.K.M., P.R., and M.P.; Software: M.M., A.Z., M.P., M.U., and A.B.S.; Validation: M.M., M.U., P.R., A.Z., N.K.M., S.R., and A.B.S.; Formal analysis: M.M., A.Z., A.H., A.N., and N.K.M.; Investigation: M.M., A.Z.; M.P., N.K.M., and M.U.; Resources: A.Z., P.R., A.B.S., and M.M.; Data curation: M.M., A.Z., A.N., N.K.M., and P.R.; Visualization: M.M., P.R., A.N., N.M.K., and S.R.; Writing – original draft: M.M., A.H., A.Z., M.P., P.R., and N.K.M.; Writing – review and editing: A.Z., K.C., M.M., and M.U.; Supervision: S.R. and M.U.; Project administration: A.Z. and M.M. All authors have read and agreed to the published version of the manuscript.

References

1. Antar, S.A.; Ashour, N.A.; Sharaky, M.; Khattab, M.; Ashour, N.A.; Zaid, R.T.; Roh, E.J.; Elkamhawy, A.; Al-Karmalawy, A.A. Diabetes Mellitus: Classification, Mediators, and Complications; A Gate to Identify Potential Targets for the Development of New Effective Treatments. *Biomedicine & Pharmacotherapy* **2023**, *168*, 115734, doi:10.1016/j.biopha.2023.115734.
2. Poznyak, A.; Grechko, A.V.; Poggio, P.; Myasoedova, V.A.; Alfieri, V.; Orekhov, A.N. The Diabetes Mellitus–Atherosclerosis Connection: The Role of Lipid and Glucose Metabolism and Chronic Inflammation. *IJMS* **2020**, *21*, 1835, doi:10.3390/ijms21051835.
3. Ojo, O.A.; Ibrahim, H.S.; Rotimi, D.E.; Ogunlakin, A.D.; Ojo, A.B. Diabetes Mellitus: From Molecular Mechanism to Pathophysiology and Pharmacology. *Medicine in Novel Technology and Devices* **2023**, *19*, 100247, doi:10.1016/j.medntd.2023.100247.
4. Yang, X.; Sun, J.; Zhang, W. Global Trends in Burden of Type 2 Diabetes Attributable to Physical Inactivity across 204 Countries and Territories, 1990-2019. *Front. Endocrinol.* **2024**, *15*, 1343002, doi:10.3389/fendo.2024.1343002.
5. FLORES-GUTIéRREZ, C.A.; Dheni TORRES-SáNCHEZ, E.; Reyes-Uribe, E.; Torres-Jasso, J.H.; Salazar-Flores, J. The Role of Pesticides in the Pathogenesis of Diabetes: A Review of Possible Mechanisms. *BIOCELL* **2025**, *49*, 767–787, doi:10.32604/biocell.2025.062225.
6. Zhao, L.; Liu, Q.; Jia, Y.; Lin, H.; Yu, Y.; Chen, X.; Liu, Z.; Li, W.; Fang, T.; Jiang, W.; et al. The Associations between Organophosphate Pesticides (OPs) and Respiratory Disease, Diabetes Mellitus, and Cardiovascular Disease: A Review and Meta-Analysis of Observational Studies. *Toxics* **2023**, *11*, 741, doi:10.3390/toxics11090741.
7. Mnif, W.; Hassine, A.I.H.; Bouaziz, A.; Bartegi, A.; Thomas, O.; Roig, B. Effect of Endocrine Disruptor Pesticides: A Review. *IJERPH* **2011**, *8*, 2265–2303, doi:10.3390/ijerph8062265.
8. Raj, A.; Kumar, A.; Khare, P.K. The Looming Threat of Profenofos Organophosphate and Microbes in Action for Their Sustainable Degradation. *Environ Sci Pollut Res* **2024**, *31*, 14367–14387, doi:10.1007/s11356-024-32159-7.

9. Wang, K.; Huang, H.; Zhan, Q.; Ding, H.; Li, Y. Toll-like Receptors in Health and Disease. *MedComm* **2024**, *5*, e549, doi:10.1002/mco2.549.
10. Onaolapo, M.C.; Alabi, O.D.; Akano, O.P.; Olateju, B.S.; Okeleji, L.O.; Adeyemi, W.J.; Ajayi, A.F. Lecithin and Cardiovascular Health: A Comprehensive Review. *Egypt Heart J* **2024**, *76*, 92, doi:10.1186/s43044-024-00523-0.
11. Zang, Y.; Wang, T.; Xie, W.; Wang-Fischer, Y.; Getty, L.; Han, J.; Corkey, B.E.; Guo, W. Regulation of Acetyl CoA Carboxylase and Carnitine Palmitoyl Transferase-1 in Rat Adipocytes. *Obesity Research* **2005**, *13*, 1530–1539, doi:10.1038/oby.2005.188.
12. Diaa Subhi, M.; Abdul Wadood AL-Shammaree, S. Evaluation of Paraoxonase-1 Activity of Arylesterase and Lactonase and Their Correlation with Oxidative Stress in Children with Type 1 Diabetes Mellitus. *rbmb.net* **2024**, *13*, 301–309, doi:10.61186/rbmb.13.3.301.
13. Adiga, U.; Banawalikar, N.; Menambath, D.T. Association of Paraoxonase 1 Activity and Insulin Resistance Models in Type 2 Diabetes Mellitus: Cross-Sectional Study. *Journal of the Chinese Medical Association* **2022**, *85*, 77–80, doi:10.1097/JCMA.0000000000000665.
14 Lee, A.Y.; Christensen, S.M.; Duong, N.; Tran, Q.-A.; Xiong, H.M.; Huang, J.; James, S.; Vallabh, D.; Talbott, G.; Rose, M.; et al. Sirt3 Pharmacologically Promotes Insulin Sensitivity through PI3/AKT/mTOR and Their Downstream Pathway in Adipocytes. *IJMS* **2022**, *23*, 3740, doi:10.3390/ijms23073740.
15. Sakinah, E.N.; Athoillah, N.; Putri, K.Y.W.; Armiyanti, Y. In Silico Determination of Fenthion, Permethrin, and Carbaryl as FFAR2 Inhibitors: Type 2 Diabetes Mellitus Pathomechanism Study. *JKKI* **2023**, 236–247, doi:10.20885/JKKI.Vol14.Iss3.art3.
16. Kouranov, A. The RCSB PDB Information Portal for Structural Genomics. *Nucleic Acids Research* **2006**, *34*, D302–D305, doi:10.1093/nar/gkj120.
17. The UniProt Consortium UniProt: A Hub for Protein Information. *Nucleic Acids Research* **2015**, *43*, D204–D212, doi:10.1093/nar/gku989.
18. Baroroh, S.Si., M.Biotek., U.; Muscifa, Z.S.; Destiarani, W.; Rohmatullah, F.G.; Yusuf, M. Molecular Interaction Analysis and Visualization of Protein-Ligand Docking Using Biovia Discovery Studio Visualizer. *IJCB* **2023**, *2*, 22, doi:10.24198/ijcb.v2i1.46322.
19. Jendele, L.; Krivak, R.; Skoda, P.; Novotny, M.; Hoksza, D. PrankWeb: A Web Server for Ligand Binding Site Prediction and Visualization. *Nucleic Acids Research* **2019**, *47*, W345–W349, doi:10.1093/nar/gkz424.
20. Tian, W.; Chen, C.; Lei, X.; Zhao, J.; Liang, J. CASTp 3.0: Computed Atlas of Surface Topography of Proteins. *Nucleic Acids Research* **2018**, *46*, W363–W367, doi:10.1093/nar/gky473.
21. Kim, S.; Chen, J.; Cheng, T.; Gindulyte, A.; He, J.; He, S.; Li, Q.; Shoemaker, B.A.; Thiessen, P.A.; Yu, B.; et al. PubChem 2023 Update. *Nucleic Acids Research* **2023**, *51*, D1373–D1380, doi:10.1093/nar/gkac956.
22. García-Valverde M, Cordero NA, de la Cal ES. GAUSSVIEW® as a tool for learning organic chemistry. InEDULEARN15 proceedings 2015 (pp. 4366-4370). IATED
23. Frisch, A. Gaussian 09W Reference; Wallingford, USA, 2009; p. 25, p. 470.
24. O'boyle, N.M.; Tenderholt, A.L.; Langner, K.M. Cclib: A Library for Package-independent Computational Chemistry Algorithms. *J Comput Chem* **2008**, *29*, 839–845, doi:10.1002/jcc.20823.
25. Dallakyan, S.; Olson, A.J. Small-Molecule Library Screening by Docking with PyRx. In *Chemical Biology*; Hempel, J.E., Williams, C.H., Hong, C.C., Eds.; Methods in Molecular Biology; Springer New York: New York, NY, 2015; Vol. 1263, pp. 243–250 ISBN 978-1-4939-2268-0.
26. Daina, A.; Michielin, O.; Zoete, V. SwissADME: A Free Web Tool to Evaluate Pharmacokinetics, Drug-Likeness and Medicinal Chemistry Friendliness of Small Molecules. *Sci Rep* **2017**, *7*, 42717, doi:10.1038/srep42717.
27. Al-Ahliyya Amman University; Azzam, K.A. SwissADME and pkCSM Webservers Predictors: An Integrated Online Platform for Accurate and Comprehensive Predictions for In Silico ADME/T Properties of Artemisinin and Its Derivatives. *KIMS/CUMR/MShKP* **2023**, *325*, 14–21, doi:10.31643/2023/6445.13.
28. Chandran, K.; Shane, D.I.; Zochedh, A.; Sultan, A.B.; Kathiresan, T. Docking Simulation and ADMET Prediction Based Investigation on the Phytochemical Constituents of Noni (Morinda Citrifolia) Fruit as a Potential Anticancer Drug. *In Silico Pharmacol.* **2022**, *10*, 14, doi:10.1007/s40203-022-00130-4.
29. Priya M, Zochedh A, Chandran K, Arumugam K, Banu S, Chakaravarthy C, Sultan AB. Computer-aided analysis of biochanin-a as a potential breast cancer drug based on dft, molecular docking, and pharmacokinetic studies. Letters in Applied NanoBioScience. 2022;12(4):165. doi: https://doi.org/10.33263/LIANBS124.165
30. Priya, M.; Arumugam, K.; Chakaravarthy, C.; Chandran, K.; Sultan, A.B.; Zochedh, A. Graph Theory Network, Molecular Docking, Quantum Chemicals and Pharmacokinetics-Based Investigation on Phytochemicals

from *Sida Rhombifolia* against Alzheimer's Disease. *Polycyclic Aromatic Compounds* **2024**, *44*, 1947–1970, doi:10.1080/10406638.2023.2209259.
31. Zochedh, A.; Chandran, K.; Priya, M.; Sultan, A.B.; Kathiresan, T. Molecular Simulation of Naringin Combined with Experimental Elucidation – Pharmaceutical Activity and Molecular Docking against Breast Cancer. *Journal of Molecular Structure* **2023**, *1285*, 135403, doi:10.1016/j.molstruc.2023.135403.
32. Sukumaran, S.; Zochedh, A.; Viswanathan, T.M.; Sultan, A.B.; Kathiresan, T. Theoretical Investigation of 5-Fluorouracil and Tamoxifen Complex – Structural, Spectrum, DFT, ADMET and Docking Simulation. *Polycyclic Aromatic Compounds* **2023**, *43*, 9443–9460, doi:10.1080/10406638.2022.2164018.
33. Zochedh, A.; Priya, M.; Shunmuganarayanan, A.; Thandavarayan, K.; Sultan, A.B. Investigation on Structural, Spectroscopic, DFT, Biological Activity and Molecular Docking Simulation of Essential Oil Gamma-Terpinene. *Journal of Molecular Structure* **2022**, *1268*, 133651, doi:10.1016/j.molstruc.2022.133651.
34. Chandran, K.; Zochedh, A.; Sultan, A.B.; Kathiresan, T. Observations into Quantum Simulation, Spectroscopy, Electronic Properties, Pharmacokinetics and Molecular Docking Analysis of Lawsone against Breast Cancer. *Journal of Molecular Structure* **2023**, *1293*, 136280, doi:10.1016/j.molstruc.2023.136280.
35. Zochedh, A.; Priya, M.; Shunmuganarayanan, A.; Sultan, A.B.; Kathiresan, T. Antitumor and Antimicrobial Effect of Syringic Acid Urea Cocrystal: Structural and Spectroscopic Characterization, DFT Calculation and Biological Evaluation. *Journal of Molecular Structure* **2023**, *1282*, 135113, doi:10.1016/j.molstruc.2023.135113.
36. Priya, M.; Zochedh, A.; Palaniyandi, K.; Shunmuganarayanan, A.; Sultan, A.B. Combinatorial Effect of Syringic Acid-Pyrazinamide Adduct against Luminal Type Breast Cancer Investigated through DFT, Drug-Likeness, and Molecular Docking Simulation. *Polycyclic Aromatic Compounds* **2024**, *44*, 2090–2118, doi:10.1080/10406638.2023.2212105.
37. Mohan, Y.S.; Zochedh, A.; Muthupandi, N.K.; Chandran, K.; Sultan, A.B. Screening of Bioactive Phytochemicals from Abutilon Theophrasti and Molecular Simulation Studies of Myricetin Targeting TGF-β Against Gastric Cancer. *Chemistry Africa* **2025**, *8*, 255–272, doi:10.1007/s42250-024-01156-1.
38. Chandran, K.; Zochedh, A.; Rawat, R.; Eyupoglu, V.; Sultan, A.B.; Kathiresan, T. Prediction of ESR1 Network and Molecular Modeling Analysis of Bioactive Molecules from Ficus Microcarpa Targeting ER-Alpha for Breast Cancer Therapy. *Chemistry Africa* **2025**, *8*, 167–186, doi:10.1007/s42250-024-01148-1.
39. Priya, M.; Zochedh, A.; Mohan, Y.S.; Chandran, K.; Arumugam, K.; Sultan, A.B. Network Analysis and Molecular Modeling Studies of Pinocembrin a Bioactive Phytochemical of Dodonaea Viscosa against Parkinson's Disease. *In Silico Pharmacol.* **2024**, *12*, 91, doi:10.1007/s40203-024-00268-3.
40. Chedik, L.; Mias-Lucquin, D.; Bruyere, A.; Fardel, O. In Silico Prediction for Intestinal Absorption and Brain Penetration of Chemical Pesticides in Humans. *IJERPH* **2017**, *14*, 708, doi:10.3390/ijerph14070708.
41. El-Nahhal, Y.; Radwan, A.; Radwan, A.M. Human health risks: Impact of pesticide application. *J. Environ. Earth Sci.* **2013**, *3*(7), 199–209.
42. Zochedh, A.; Chandran, K.; Shunmuganarayanan, A.; Sultan, A.B. Exploring the Synergistic Effect of Tegafur-Syringic Acid Adduct Against Breast Cancer through DFT Computation, Spectroscopy, Pharmacokinetics and Molecular Docking Simulation. *Polycyclic Aromatic Compounds* **2024**, *44*, 2153–2187, doi:10.1080/10406638.2023.2214281.
43. Kushwaha, M.; Verma, S.; Chatterjee, S. Profenofos, an Acetylcholinesterase-Inhibiting Organophosphorus Pesticide: A Short Review of Its Usage, Toxicity, and Biodegradation. *J of Env Quality* **2016**, *45*, 1478–1489, doi:10.2134/jeq2016.03.0100.
44. Dasu, M.R.; Ramirez, S.; Isseroff, R.R. Toll-like Receptors and Diabetes: A Therapeutic Perspective. *Clinical Science* **2012**, *122*, 203–214, doi:10.1042/CS20110357.